Multiple electromagnetic excitations of relativistic projectiles

W. J. Llope and P. Braun-Munzinger
Department of Physics, State University of New York at Stony Brook, Stony Brook, New York 11794
(Received 27 August 1991)

Conditions optimum for the first experimental verification of the multiple electromagnetic excitations of nuclei in relativistic nucleus-nucleus collisions are described. The relative magnitudes of three important physical processes that might interfere with such a measurement are compared to the predicted strengths for the single and multiple electromagnetic excitations for various choices of the projectile mass and beam energy. Strategies are presented for making inferences concerning the presence of multiple excitation strength in experimental data.

PACS number(s): 25.75.+r

I. INTRODUCTION

Multiple electromagnetic excitations of relativistic nuclei to excitation energies above ~20 MeV may result in intermediate and final nuclear states that are not accessible by any other means. The multiple excitation process of interest in this work involves the simultaneous absorption of (equivalent) photons into the giant dipole resonance (GDR) during Coulomb interactions between relativistic nuclei—producing states of high excitation energies and large isospin quantum numbers, but small temperatures. The existence of such exotic large-amplitude collective states in nuclei has yet to be experimentally verified even though a fairly large body of data has been collected [1–9]. We note, though, an indication of the excitation of double GDR states in pion double charge exchange reactions [10], and an interpretation of high energy structures in the excitation energy spectra in ^{208}Pb targets following inelastic collisions with various projectiles in terms of multiphonon excitations [11], although these structures were not reproduced in subsequent measurements [12]. Very little is known from an experimental or theoretical perspective concerning the decay of multiple GDR states.

Experimental investigations of the dissociation of relativistic nuclei following electromagnetic interactions have been completed by several groups [1–9]—providing solid evidence for the interpretation of the dominant part of the measured dissociation cross sections as first-order excitations followed by the statistical decay of the excited nucleus [13]. The cross sections for these first-order excitations are accurately reproduced by calculations involving the Weizsäcker-Williams approximation [14–16], coupled with experimentally measured photoabsorption cross sections [17–18] over the full range of nuclei, final states, and beam energies studied.

Recently, calculations predicting the fragmentation cross sections following the single and multiple excitation of light, self-conjugate nuclei at Brookhaven National Laboratory–Alternating Gradient Synchrotron (BNL-AGS) energies ($E_{\rm proj}$ = 14.6 GeV/nucleon) were published [13]. These predictions for multistep excitations were obtained in a Weizsäcker-Williams framework which employed the experimentally measured total photoabsorption cross sections to describe the nuclear response to the electromagnetic interaction. While the cross sections for first-order excitations scale with the target charge approximately like $\sigma \sim Z_T^2$, dissociations following the absorption of exactly n photons scale approximately like $\sigma \sim Z_T^{2n}$. The geometry of the colliding nuclei and the impact parameter dependence of the excitation probabilities actually make these exponents slightly less than the exactly Z_T^{2n} dependence expected from the Weizsäcker-Williams equivalent photon spectra.

Comparison with previously published and more schematic methods used for the calculation of multiple excitation strength functions [19] indicate an important physical process that must be considered during any attempt to make the first experimental verification of multiple electromagnetic excitations. According to calculations performed with the model described in Ref. [13], a significant "background" to the multiple electromagnetic excitations is provided by first-order absorption to the same nuclear excitation energies covered by the higher-order processes. Thus, even if multiple GDR states have narrow widths (i.e., on the order of the first-order GDR), their differential excitation probability is, in general, much smaller than what is predicted for first-order excitation by the absorption of the (virtual) photon on a quasideuteron, a correlated n-p pair within the (projectile) nucleus [20].

One possibility for experimental verification of the multiple electromagnetic excitation process is thus to resort to very accurate measurement of the excitation spectrum near the peak of the expected multiple excitation strength functions [13]. Rather than measuring the excitation spectra directly, however, one could also make inferences about the multiple excitation process by inspecting the cross sections for dissociation into decay channels open for excitation energies where multiple GDR excitation and decay is expected to occur. Although the particle decay probability of multiple GDR states cannot presently be accurately predicted, the primary excitation spectrum can nonetheless be inferred from such measurements if one considers the ratios of cross sections for projectile fragmentation by different targets.

First-order electromagnetic excitations, however, are not the only physical processes competing with multiple excitations. In collisions in which the impact parameter b is approximately the sum of the nuclear radii, interactions involving the nuclear field become an important source of excitation strength. The most peripheral of these hadronic interactions may result in final states similar to those populated by electromagnetic interactions [1]. In addition, while the photoexcitation of giant quadrupole states—both isoscalar and isovector—may not exhaust large fractions of the relevant sum rule strengths, such excitations may provide significant contributions to the overall cross sections [21–23].

The importance of each of these competing processes relative to the predicted strengths of single and multiple electromagnetic excitations may be strongly dependent on the beam energy or the projectile/target combination, for example. Motivated by the availability of new experimental data both from experiments [24,25] at the AGS at BNL and the SIS accelerator at GSI, providing projectile nuclei with beam kinetic energies of 14.6 GeV/nucleon and ~1 GeV/nucleon, respectively, we investigated the relative magnitudes of the electromagnetic and competitive nuclear excitation probabilities for the various projectile masses or beam energies of interest. Initial results of calculations performed for the dissociation by a variety of targets of a light projectile, ^{28}Si, at the relatively large beam energies available at the AGS have already been published [13]. Herein, we extend the predictions for the importance of single and multiple electromagnetic excitations, against the backdrop of competitive physical processes, to the case of a heavy projectile at relatively low beam energies—^{136}Xe at 0.65 GeV/nucleon. To stay close to experiment, we will give an overview of predictions for the strengths of multiple electromagnetic excitations and compare them to those arising from competitive processes for varying choices of the nuclear species and kinematic conditions. The results of these calculations should provide a benchmark against which to compare recently collected experimental data [24, 25].

II. COMPETITIVE PROCESSES

In Ref. [13], we introduced a method to compute multiple electromagnetic excitation probabilities by combining the Weizsäcker-Williams method with a realistic description of (real) photon absorption. In this model, multistep excitations are obtained by the convolution of the probability for single-step excitations from the ground state of the projectile nucleus. The assumption of the harmonicity of the collective potential results in quantitative calculations that indicate that the strength function for the nth-order excitation of a GDR state of mean energy $E_{\rm GDR}$ and width $\Gamma_{\rm GDR}$ has a mean energy of $E^{(n)} = nE_{\rm GDR}$, and a width of $\Gamma^{(n)} \sim \frac{3}{2}n\Gamma_{\rm GDR}$ for light nuclei and $\Gamma^{(n)} = n\Gamma_{\rm GDR}$ for (heavy) nuclei characterized by Lorentzian photoabsorption cross sections. Experimentally measured dissociation cross sections are accurately reproduced by our model when including only first-order excitations, and decay probabilities given by the standard statistical model, in the calculation.

We stress, however, that this semiclassical approach, in which the probabilities for multiple excitations are given by Poisson distributions in the probability for first-order excitations, does *not* consider effects such as, for example, quantum-mechanical interference in the excitation process. We also acknowledge that the probability for higher-order electromagnetic excitations can be influenced by the detailed microscopic structure of multiply excited GDR states, which is entirely neglected in the present approach.

At present, no experimental data have been published for electromagnetic dissociations in relativistic nucleus-nucleus collisions that could corroborate, by way of cross-section ratios, our predictions for multiple excitation strengths. Experimental data are available [3, 4] for the electromagnetic dissociation of a variety of nuclei at beam energies near 1 GeV/nucleon, but only for dissociation into those final states (generally the $1n$ and $2n$ channels) that are of negligible importance for excitation energies where the multistep GDR excitations are expected to contribute. Decay strength in excess of that calculated in a purely first-order Weizsäcker-Williams framework in the $^{32}S^* \rightarrow {}^{28}$Si + α reaction, measured [9] in emulsions, was attributed to two-photon absorption, but an interpretation of this excess in terms of nuclear excitations is more plausible given the expected excitation energy dependence of multiple electromagnetic excitations and the role of isospin in the reaction. Cross-section ratios produced [13] following the measurement [1] of the dissociation of ^{28}Si at 14.6 GeV/nucleon by the E814 Collaboration [24] did not have sufficient statistical accuracy to establish the presence or absence of multiple excitations. Data from a subsequent high statistics run by this group are presently being analyzed, while an experiment [25] at the SIS accelerator at GSI has recently collected data for the dissociation of ^{136}Xe at kinetic energies of 0.65 GeV/nucleon.

In our view, the folding model [13] includes the physics of the excitation process necessary for a quantitative comparison with experiment, with the caveats mentioned above. Predictions using our model indicate that the individual strengths for the absorption of a specific number of (equivalent) photons are distinct, but are usually only a fraction of the strength of first-order excitations. Therefore, some consideration of the relative magnitudes of the following competitive physical processes is necessary during the analysis of existing data, or the collection of new data, before inferences concerning the presence of multiple excitation strength will be possible.

A. First-order excitations

The Weizsäcker-Williams number spectrum [15, 16], proven in many studies to describe the photon flux seen by the projectile in these extremely peripheral collisions [1, 21], contains a continuum of photon energies up to a certain adiabatic cutoff. This cutoff is linear in the Lorentz boost of the projectile, γ_P, and is given by

$$E_\gamma^{\rm max} \sim \frac{\hbar c \gamma_P \beta_P}{b_{\rm min}}, \quad (1)$$

where $b_{\min}$ is the smallest impact parameter for which interactions involving the nuclear field are negligible. At the AGS ($E_{\rm proj}$ = 14.6 GeV/nucleon) or the Super Proton Synchrotron (SPS) at CERN ($E_{\rm proj}$ = 60, 200 GeV/nucleon), adiabaticity in the Weizsäcker-Williams number spectra for ^{28}Si on ^{208}Pb occurs at roughly $E_\gamma^{\max} \sim 350$ MeV for the AGS, and 1.2 and 4 GeV, respectively, for the SPS. These adiabatic cutoffs are roughly a factor of 2 higher in photon energy for ^{28}Si on ^{12}C. Previously [13], we found that the strengths of multiple electromagnetic interactions under these conditions are always dominated by first-order excitations to the same excitation energy, principally through absorption by the quasideuteron mechanism [20].

However, at lower beam energies, the adiabaticity in the Weizsäcker-Williams number spectrum can be exploited to suppress the background to the multiple electromagnetic excitations from the first-order processes that dominate excitations at facilities with higher beam energies. Requiring that the adiabatic cutoff occurs below the excitation energies covered by double-GDR states, but above the first-order GDR, yields a range of beam energies optimum for maximizing the importance of double-GDR excitations relative to single-GDR excitations given by the following simple relation:

$$E_{\rm GDR} + \Gamma_{\rm GDR} \lesssim \frac{\hbar c \gamma_P \beta_P}{b_{\min}} \lesssim 2E_{\rm GDR} - \Gamma_{\rm GDR}. \qquad (2)$$

Here, $E_{\rm GDR}$ and $\Gamma_{\rm GDR}$ are the mean energy and width of the giant dipole resonance, which dominates the photoabsorption by the projectile nucleus. We note that, for simplicity, the upper limit in the above is calculated using the width of the single GDR. For such relatively low beam energies (specified by the range of choices for γ_P above), the contribution of excitation strength from first-order processes in the region of excitation energies covered by the multiple excitation strength is strongly suppressed, while still providing a significant probability for (single) GDR excitation.

To quantify this point, we take the mean GDR energy and width from a hydrodynamical model prediction [26] and plot the projectile laboratory kinetic energies implied by equation (2) as a function of the projectile mass in Fig. 1. In this plot, the ranges of beam energies that satisfy Eq. (2) are shaded; the differences between the ranges of beam kinetic energies implied for the ^{12}C and ^{208}Pb targets are due to the target dependent choice for the quantity $b_{\min}$, which is made as described in Sec. III.

Thus, the excitation strength in first-order electromagnetic excitations that competes with multiple electromagnetic excitation strengths is strongly suppressed by the adiabaticity imposed by a rather wide range of relatively low beam energies. In this paper, we will compute as an example the excitation of ^{136}Xe projectiles at 0.65 GeV/nucleon. Such a choice [25], marked as a crossed point in this figure, is well suited for the suppression of first-order electromagnetic excitations by heavy targets near the double GDR.

At such low beam energies, the "background" to multiple excitations arising from first-order excitations is suppressed. However, one must also pay the price of smaller overall excitation cross sections as compared to those possible with higher beam energies. Thus, if the only process that might interfere with the measurement of multiple excitation strength was first-order electromagnetic excitations, the best choice of the beam energy would be one that is somewhat above the curves shown in Fig. 1, maximizing the photon flux in energies covered by the (first-order) giant dipole resonance, while still suppressing first-order excitations to the energies covered by the expected higher-order GDR's.

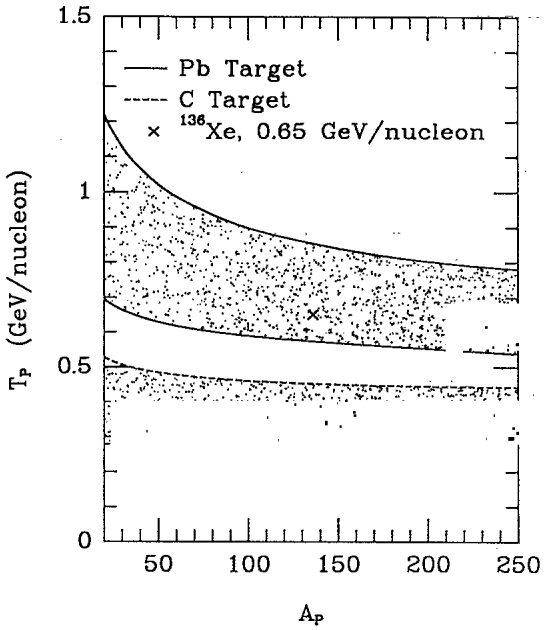

FIG. 1. The range of laboratory projectile kinetic energies that is optimum for the suppression of first-order excitations of the projectile in the region of excitation energies covered by higher-order excitations, as a function of the projectile mass for C (dashed lines) and Pb (solid lines) targets.

First-order interactions involving the absorption $E1$ photons, however, are not the only electromagnetic processes that compete with multiple GDR excitations. In the next section, we discuss the role of another important electromagnetic excitation process—that involving the excitation of giant quadrupole resonances (GQR's) following the absorption of $E2$ (equivalent) photons.

B. Giant quadrupole excitations

The Weizsäcker-Williams pulse of plane polarized radiation that is assumed to approximate the effect of the Coulomb field of a nucleus during an electromagnetic interaction contains equivalent photons of all multipolarities. In this section, we provide estimates for the contributions to the overall strengths from excitations following the absorption of photons with multipolarity other than $E1$.

The Weizsäcker-Williams number spectra, $n_{\pi\lambda}$, depend on the multipolarity $\pi = E$ (electric) or M (magnetic), angular momentum λ, energy E_γ, and impact pa-

rameter b of the collision, as well as the beam energy. All number spectra approach $n_{E1}(E_\gamma, b)$ in magnitude as the beam energy approaches infinity [16]. The most probable absorptions not involving $E1$ photons involve the absorption of quadrupole radiation, populating both isoscalar (ISGQR) and isovector (IVGQR) giant quadrupole resonances.

These resonances occur at a mean energy given approximately by

$$E_{\mathrm{GQR}} \sim \frac{E_0}{A^{1/3}} \ \mathrm{MeV}, \tag{3}$$

where $E_0 \sim 63$ (125) MeV for the isoscalar [27] (isovector [28]) GQR. A value of E_0 for the isovector GQR ranging from 120 to 130 MeV has been cited in later reviews [29]. Thus, the isoscalar GQR provides additional absorption strength in a region of excitation energies covered by first-order $E1$ excitations. The isovector GQR is higher in the continuum, perhaps providing absorption strength that will interfere with the measurement of the strength in multiple $E1$ excitations, as first discussed by Pruneau and Takai [23].

At beam energies near 1 GeV/nucleon, $E2$ equivalent photons are far more plentiful than $E1$ photons [16, 19]. Previously published calculations [19, 21] have indicated that the photoexcitation of giant quadrupole resonances decreases in importance, with the decreasing number of $E2$ compared to $E1$ photons, as the projectile energy increases. Thus, the "background" to single and multiple $E1$ excitations resulting from electromagnetic excitations of giant quadrupole resonances is most troublesome at the lower beam energies implied by Sec. II A.

To investigate the integrated strengths and possible excitation energy dependence of GQR excitations compared to first- and second-order GDR states, we start with the experimental total cross section for the absorption of real photons by the projectile nucleus. We then parametrize the differential photoabsorption cross section for the excitation of isoscalar and isovector GQR's as Lorentzians in three parameters—the mean energy, width, and fractional exhaustion of the relevant oscillator sum rule (FESR). Since the total photoabsorption cross section contains the strengths for absorptions of predominately $E1$ and $E2$ photons, the parametrization of the photoabsorption cross section leading to GQR states then determines the strength function for the absorption of purely $E1$ photons—the mean energy, width, and integral of which should be consistent with experimental measurements of the GDR and the $E1$ sum rule [29]. These parametrizations will allow predictions for the differential excitation cross sections for states following $E2$ absorptions and direct comparison with the differential excitation strengths expected of $E1$ absorptions of various orders.

Calculations predicting the cross sections for the excitation of giant quadrupole resonances, especially in the context of their magnitude with respect to $E1$ excitations, have been performed previously by several groups [21, 23]. These predictions also involved the construction of the GQR photoabsorption cross sections from Lorentzians, the parameters for which were taken either directly from available experimental data [29, 30] or from the systematics implied by these data.

We note that considerable extrapolation is necessary to obtain the parameters for the isovector GQR photoabsorption cross section in ^{28}Si; the lightest nuclei for which IVGQR strength has been identified [29] are ^{56}Fe and ^{58}Ni, for which $\Gamma \sim 9$ MeV and only (11±1)% of the isovector GQR sum-rule strength was identified. This extrapolation would imply the absence of isovector GQR strength in ^{28}Si. We thus expect that the photoexcitation of isovector GQR's is important only in heavy nuclei, but we nonetheless allow a FESR of the isovector GQR sum rule of 1% for ^{28}Si from the systematics for purposes of comparison. Thus, we assume that the isoscalar GQR could be described with $\Gamma \sim 4.5$ MeV (5.1 MeV) and FESR=70% (30%), while the isovector GQR would have $\Gamma \sim 7$ MeV (10 MeV) and FESR$\sim$80% ($\lesssim$1%), for ^{136}Xe (^{28}Si) nuclei.

A large body of experimental data on the centroids, widths, and total strengths relative to the sum rule for isoscalar GQR's exist in the literature [29]. However, due to the freedom in the assignment of the parameters allowed by the systematics of a very limited amount of experimental data in the case of the isovector GQR, we provide in addition to parametrizations based on the systematics those possible in a "worst-case" scenario. By taking a relatively narrow width of 5 MeV and complete exhaustion of the relevant sum rule for both GQR states, estimates for the maximum possible contribution to the excitation strengths from $E2$ absorptions will be obtained.

The photoabsorption cross sections for isoscalar and isovector GQR states in ^{136}Xe and ^{28}Si used herein are depicted in Figs. 2. In these plots, the total photoabsorption cross section measured experimentally [17, 18] with real photons is given by the solid lines, while the parametrized isoscalar (isovector) GQR strength functions are given by the dashed (dot-dashed) lines. The GQR Lorentzians are normalized to total strengths given by the product of the classical sum rule and fractional exhaustion of this sum rule. The sum-rule strength for the isoscalar GQR is calculated as described in Ref. [28], while the Gellman-Telegdi sum rule is used for the isovector GQR:

$$\int \frac{\sigma_\gamma(E_\gamma)}{E_\gamma^2} dE_\gamma = \frac{\pi^2}{5} \frac{e^2}{\hbar c} \frac{1}{mc^2} \frac{NZ}{A} R^2, \tag{4}$$

where R is the nuclear uniform density radius, which we take as $R = 1.2A^{1/3}$, and m is the nucleon mass. Neglecting the possibility of magnetic resonance strength, the difference between the experimental total and the two GQR photoabsorption cross sections is the photoabsorption cross section for purely $E1$ photons. This is depicted as the dotted lines in Fig. 2.

To provide a comparison of the possible differential excitation cross sections for isoscalar and isovector GQR states with respect to single and multiple GDR excitations, we fold the particular photoabsorption cross section depicted in Fig. 2 with the appropriate analytic number spectrum of (equivalent) photons [16]. The differen-

tial cross sections so obtained are plotted along with the strengths in single and double $E1$ excitations, which were calculated as described in Ref. [13] and in Sec. III below, for the excitations of ^{136}Xe at 0.65 GeV/nucleon and ^{28}Si at 14.6 GeV/nucleon by ^{208}Pb targets in Figs. 3 and 4. The excitation cross sections calculated using the "worst-case" GQR photoabsorption cross sections are depicted in Figs. 3, while those obtained using the parametrizations based on the systematics are shown in Figs. 4.

The number spectra used in the calculations shown in these figures are generated using a value of $b_{\min}$ which is taken from Ref. [31], as described below. For both sets of projectile nucleus and beam energies shown in this figure, isoscalar GQR's are of negligible strength in the regions of excitation energies covered by double-GDR excitations. Any interference with the measurement of double-GDR states will thus be the result of photoabsorptions leading to isovector GQR states.

For the case of isovector GQR excitations in ^{136}Xe, Figs. 3(a) and 4(a), the maxima of the isovector GQR excitation functions calculated from both parametrizations of the GQR photoabsorption cross section lies above the predicted strength of double-GDR excitations. This indeed provides the possibility that such isovector GQR strength might be mistaken as the strength of a double-GDR state. However, most of this strength lies below the expected mean energy of the double-GDR state, which is given by $E^{(2)}_{\rm GDR} = 2E^{(1)}_{\rm GDR}$. In addition, we note that, according to both parametrizations, the isovector GQR absorption strength is least important for excitation energies covered by and above the $4n$ decay channel from ^{136}Xe.

For isovector GQR states in ^{28}Si projectiles at 14.6 GeV/nucleon, depicted in Figs. 3(b) and 4(b), the worst-case parametrization of the isovector GQR strength function would imply that the excitation cross sections for double-GDR states are completely dominated by those for absorptions leading to (first-order) isovector GQR's. However, a more realistic estimate, based on a long-range extrapolation of the systematics, implies that the background to double-GDR states imposed by isovector GQR excitations is negligible for light nuclei. This same

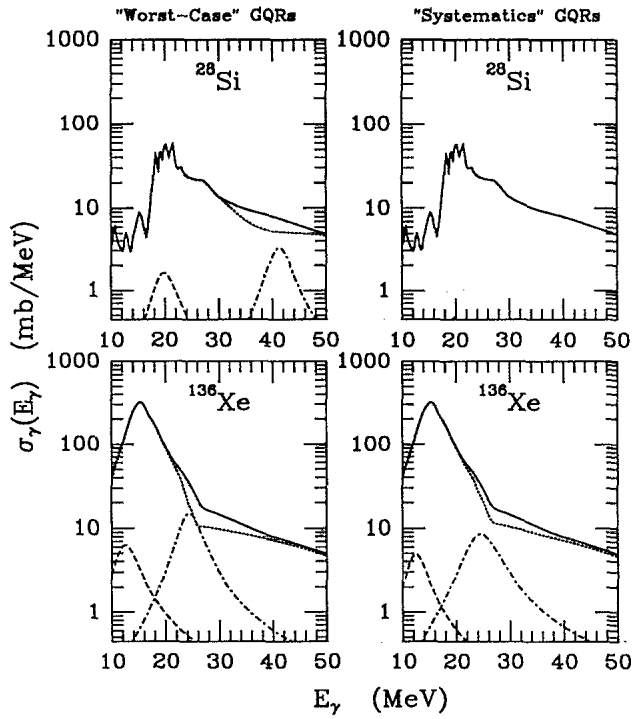

FIG. 2. The total photoabsorption cross section for ^{28}Si and ^{136}Xe nuclei (solid lines), as well as the parametrizations for the isoscalar GQR (dashed lines) and the isovector GQR (dot-dashed lines). The GQR's are each taken to be Lorentzians, the parameters for which are taken either for a "worst-case" depiction (left-most frames) or from the systematics of the available experimental data (right-most frames). The subtraction of the two GQR strength functions from the total photoabsorption cross section is then assumed to give the absorption probability for $E1$ photons (dotted lines). The "systematics" GQR's for ^{28}Si are too weak to appear in the upper-right frame.

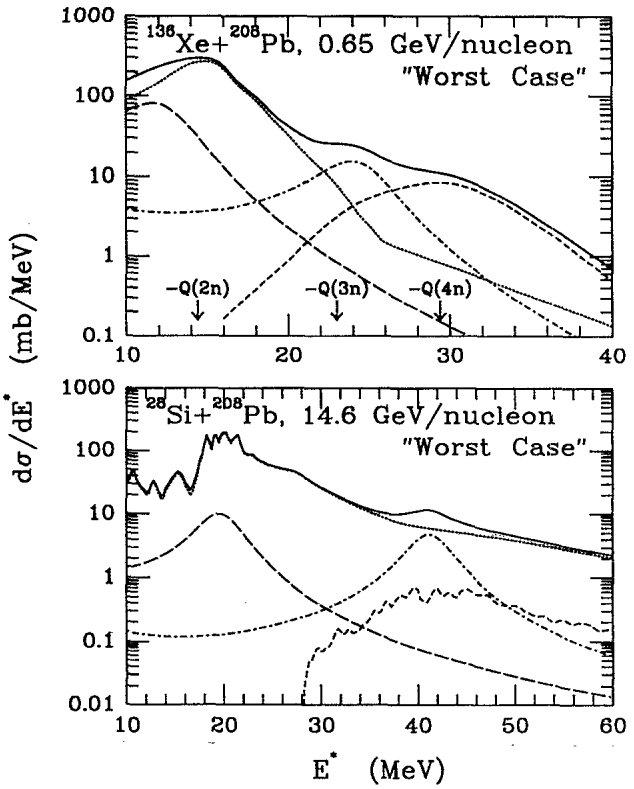

FIG. 3. The calculated differential cross sections for first-order GDR (dotted lines), second-order GDR (short-dashed lines), first-order isoscalar GQR (long-dashed lines), and first-order isovector GQR excitations (dot-dashed lines) for ^{136}Xe on ^{208}Pb at 0.65 GeV/nucleon (upper frame) and ^{28}Si on ^{208}Pb at 14.6 GeV/nucleon (lower frame). The sum of these excitation strength functions is shown as the solid line in each frame. The GQR photoabsorption cross sections are intended to depict a "worst-case" scenario following the assumption of a narrow width for these states and complete exhaustion of the relevant sum rules. The calculated threshold Q values for the $2n$, $3n$, and $4n$ decay channels from ^{136}Xe are marked. Note the different scales on the axes of the two frames.

conclusion was also reached in similar calculations by Pruneau and Takai [23].

It is relevant to compare the estimates obtained above with other estimates not sensitive to the specific choices for the parameters, and indeed the functional form itself, necessary to describe the photoabsorption cross sections leading to quadrupole resonances. We numerically integrated the various strength functions from the "worst-case" parametrizations of the two GQR strength functions, shown in Figs. 3, and compared the relative integrated strengths so obtained with those calculated as described in Ref. [19], and found agreement to better than the 1% level.

For the case of ^{136}Xe on ^{208}Pb at 0.65 GeV/nucleon, the total cross section for double-GDR excitations following multiple $E1$ absorption is about 5.1% of the total first-order $E1$ strength. This should be compared with relative strengths of approximately 17% for the isoscalar GQR and 6.2% for the isovector GQR with respect to the total first-order $E1$ absorption strength. This implies that great care is necessary for the experimental verification of multiple excitations due to the importance of $E2$ absorptions, predominately those leading to isovector GQR's, near the double GDR.

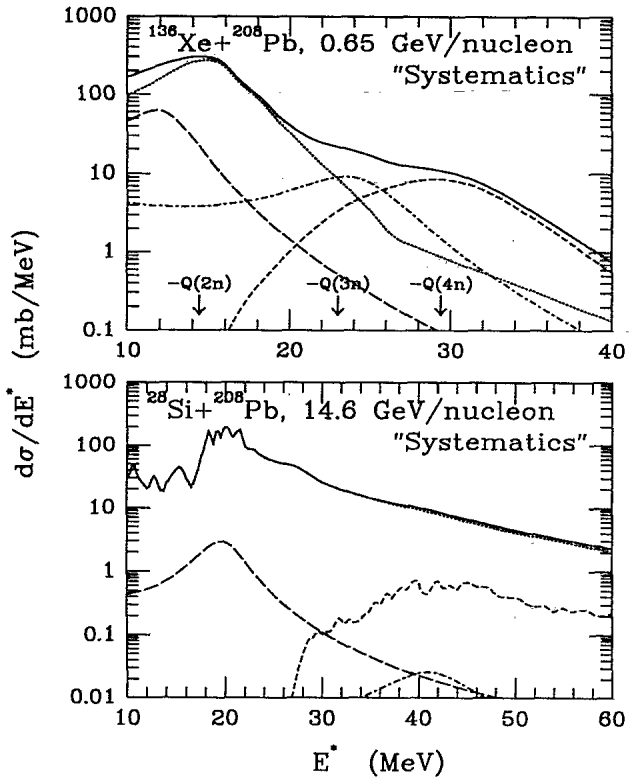

FIG. 4. The calculated differential cross sections for first-order GDR (dotted lines), second-order GDR (short-dashed lines), first-order isoscalar GQR (long-dashed lines), and first-order isovector GQR excitations (dot-dashed lines) for ^{136}Xe on ^{208}Pb at 0.65 GeV/nucleon (upper frame) and ^{28}Si on ^{208}Pb at 14.6 GeV/nucleon (lower frame). The sum of these excitation strength functions is shown as the solid line in each frame. The GQR photoabsorption cross sections were generated from the systematics of the available experimental data. The calculated threshold Q values for the $2n$, $3n$, and $4n$ decay channels from ^{136}Xe are marked. Note the different scales on the axes of the two frames.

Experimental cross sections in excess of those presented herein are thus *not* necessarily a signature of the presence of multiple excitation strength. One cannot easily infer the presence of multiple excitations from partial or differential cross sections alone. The most sensitive indications of the excitation mechanism involve the inspection of the *scaling* of the cross sections with the target charge, possible, for example, by forming the ratios of cross sections for targets with different charges.

The ratios of measured cross sections from different targets are insensitive to the multipolarity of the absorbed quanta due to the approximate Z_T^2 dependence of both $E1$ and $E2$ equivalent photon number spectra. Indeed, such cross-section ratios are enhanced by multiphoton absorption *whether these photons are both $E1$ in nature or some combination of $E1$ and $E2$ photons.* Thus, while the inspection of experimentally measured cross sections may indicate important sources of absorption strength from $E2$ photons leading to the excitation and decay of isoscalar and isovector GQR's, these (first-order) $E2$ excitations "drop out" of cross-section ratios, leaving visible enhancements caused only by multistep excitations. We note that the relative magnitude of the integrated strengths for $E1$ and the two types of $E2$ excitations implies that the multiple excitation of giant quadrupole resonances can be neglected compared to multiple $E1$ excitations, although the calculation of multiple GQR states would be possible after a straightforward extension of the framework described in Ref. [13].

While the use of low beam energies conveniently suppresses first-order excitations near the predicted multistep GDR strength functions, it concomitantly enhances the contribution of isoscalar and isovector GQR excitations relative to single and multiple GDR strength as compared to larger beam energies. In the next section, we discuss a third physical process that may interfere with attempts to measure multiple GDR excitations—that in which projectile dissociation occurs following nuclear interactions.

C. Nuclear excitations

The probability for electromagnetic excitations decreases very quickly with increasing impact parameter. However, in collisions with impact parameters very close to the sum of the nuclear radii which provide the largest possible (single and multiple) electromagnetic excitation strength, peripheral nuclear interactions may also contribute to the fragmentation. These grazing nuclear collisions may result in final states similar to those populated by electromagnetic interactions [1], providing contamination that could, in the worst case, completely wash out indications of multiple electromagnetic excitation strength.

The impact parameter dependence of nuclear and electromagnetic excitations of ^{136}Xe by ^{208}Pb targets for beam energies appropriate to the AGS and the SIS accelerators is depicted in Figs. 5. In this plot, the differential cross section for nuclear interactions is calcu-

lated numerically in a Glauber framework, as described, for example, in Refs. [31–33]. The density distributions for ^{136}Xe and ^{208}Pb are taken as Fermi distributions, the parameters of which were taken from the results of electron-scattering experiments [34]. A slight beam energy dependence of this nuclear cross section is introduced by the variation with energy of the nucleon-nucleon total interaction cross sections [35] necessary as input to the calculation. The impact parameter dependence of the first- through fourth-order electromagnetic excitation cross sections are calculated in the framework described below and in Ref. [13]. For clarity, the horizontal axis is normalized by the parameter $b_{\min}$, which is chosen for each system as described in Sec. III.

At AGS energies, the cross sections for electromagnetic interactions extend over a wide range of impact parameters. However, at lower beam energies, the adiabaticity that conveniently suppresses first-order excitations where the higher-order strength functions are important also constrains the multistep excitations to a limited range of impact parameters very close to the sum of the nuclear radii. The higher the order of excitation, the more limited the range of impact parameters that contribute.

Thus, the quality of the separation of events resulting from nuclear interactions is of *crucial* importance for the study of (multiple) electromagnetic excitations at the low beam energies implied in Sec. II A. Contamination of the event sample by events following nuclear interactions suppresses cross-section ratios, in the worst case, washing out any indications of multiple electromagnetic excitation strength.

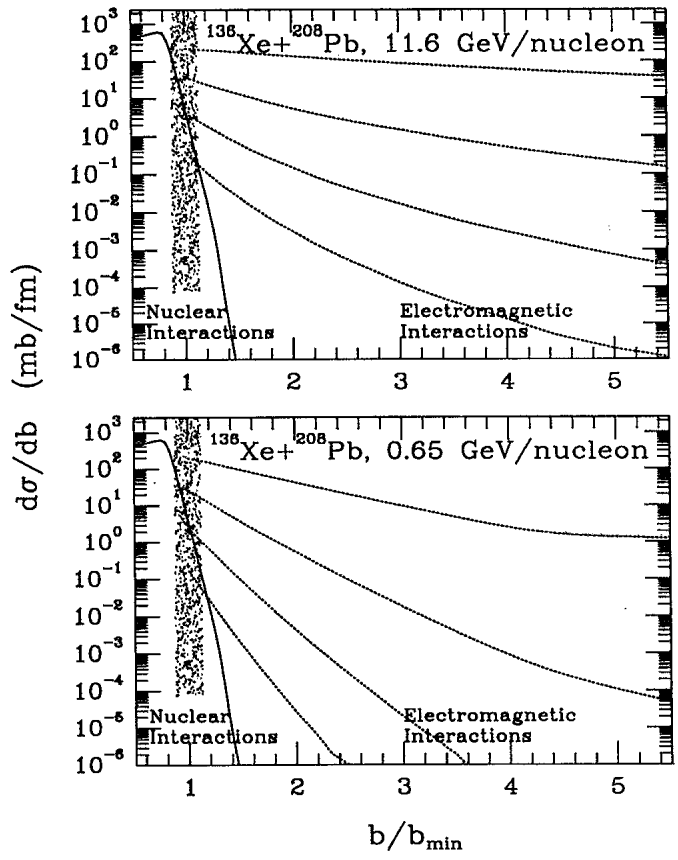

FIG. 5. The differential cross section for nuclear interactions (solid line), and the differential cross sections for first- through fourth-order electromagnetic excitations (dotted lines) as a function of the impact parameter for ^{136}Xe at beam energies appropriate for the BNL-AGS and the GSI-SIS accelerators. The shading for $b \sim b_{\min}$ is intended to underscore the experimental difficulty in the separation between electromagnetic and nuclear excitations for roughly this range of impact parameters.

III. INPUT TO THE CALCULATIONS

With predictions for the relative, beam energy and projectile species dependent, magnitudes of three important sources of "background" to the experimental measurement of multiple excitation strength in mind, we describe in greater detail (than that presented in Figs. 3, 4, and 5) the predictions of the present folding model for the (multiple) $E1$ excitation and decay of projectile nuclei at beam energies on the order of 1 GeV/nucleon. Specifically, we provide the results of our calculations for the electromagnetic dissociation of ^{136}Xe at a beam kinetic energy of 0.65 GeV/nucleon. This will then allow comparison of the predicted magnitudes of the signatures of the multiple excitation process at relatively low (SIS or Bevalac) as well as high (AGS [13]) beam energies. To make quantitative predictions using the framework of Ref. [13], the following modifications and additions were made to predict cross sections for heavy projectiles at low beam energies.

The total photoabsorption cross section for ^{136}Xe was taken as a smooth interpolation between the photoabsorption cross sections for ^{127}I, ^{133}Cs, and ^{138}Ba. These were taken from Ref. [18]. The photoabsorption cross section for ^{136}Xe is a smooth Lorentzian in shape, so the fine structure noticed in the single and multiple excitation cross sections for light nuclei like ^{28}Si will not be present [13].

To calculate the excitation cross sections for purely $E1$ excitations, the possible absorption strength in isoscalar and isovector GQR states is subtracted from the total photoabsorption cross section; this difference (shown as the dotted lines in Fig. 2) is then used as input into the present folding model. This is an important distinction from previous work [13] where, due to the near equality of the $E1$ and $E2$ number spectra for projectile energies available from the AGS, the experimentally measured total photoabsorption cross section was used without additional subtraction of the possible strengths of GQR absorptions. At the lower beam energies implied by Sec. II A, the approximation of all of the number spectra by that for $E1$ photons, coupled then with the total photoabsorption cross section measured with real photons to produce the absorption cross sections, is inaccurate.

For all of the results on pure $E1$ excitations discussed in the next section, the parameters for the Lorentzian GQR strength functions in ^{136}Xe were those taken from the systematics of the available experimental data, not the "worst-case" scenario described above. The limited sample of nuclei for which isovector GQR strength has

been identified with reasonable accuracy are all medium to heavy in weight ($A \gtrsim 60$ [29, 30]), leading to reasonably accurate interpolation of the necessary parameters for ^{136}Xe nuclei as compared to ^{28}Si. This should allow a more accurate comparison with the recently collected experimental data [25] than that possible using the "worst-case" parametrizations for the various GQR strength functions.

The necessary choice of a minimum impact parameter, $b_{\min}$, below which semihadronic excitations dominate, is made in the context of the so-called "BCV" framework [31], as stressed by Norbury and Townsend [36]. A choice of $b_{\min}$ using the relation $b_{\min} = 1.2(A_T^{1/3} + A_P^{1/3})$, as done in Ref. [13], would lead to an overall increase in the calculated first-order cross sections by about 13% for ^{136}Xe projectiles at 0.65 GeV/nucleon, and by about 3% for ^{28}Si and 14.6 GeV/nucleon. Due to the steep dependence of the electromagnetic excitation cross sections on impact parameter, visible in Figs. 5, careful choice of the parameter $b_{\min}$ is more critical for the calculation of first-order cross sections at low beam energies than at higher energies, and also more critical for the calculation of higher-order cross sections than for first-order cross sections at all beam energies.

The consideration of recoil effects for the calculation of the equivalent photon number spectra, which were neglected in our calculations performed for AGS beam energies [13], are implicit to the BCV framework and its parametrization of $b_{\min}$. In previous work [19], recoil was treated by scaling $b_{\min}$ using $b_{\min} \rightarrow b_{\min} - \pi d/2$, where d is the distance of closest approach of the two heavy ions. We note, however, that this recoil correction is quite small for relativistic projectiles, being $\lesssim 0.1$ fm, and could be neglected if $b_{\min} = R_P + R_T$ was used in our model because the overall accuracy of these calculations is not expected to be better than a few percent anyway, due to the neglection of the nuclear form factor.

A simple but approximate treatment of the nuclear form factor is possible by replacing the number spectrum $n_{\pi\lambda}(E_\gamma, b)$, which is evaluated over a range of impact parameter $b_{\min} \leq b \leq \infty$, by $\mathcal{B}(b) n_{\pi\lambda}(E_\gamma, b)$ and evaluating over the range $0 \leq b \leq \infty$. Then, as suggested by studies of nuclear inelastic scattering in the context of the optical model [28], we adopt the following form for the "start" function $\mathcal{B}$:

$$\mathcal{B}(b) = 1.0 - \frac{1}{1.0 - \exp[(b - R_P - R_T)/a]}, \qquad (5)$$

where a is the "skin thickness" of a description of the impact-parameter dependence of the nuclear cross section in terms of a Fermi distribution and the radii of the projectile and target, R_P and R_T, are each given by $R = 1.2A^{1/3}$. A complete discussion of the use of this function in our folding model is beyond the scope of this paper; we note, however, that as a first approximation to the transition from peripheral nuclear to peripheral electromagnetic interactions, implied by Fig. 5, a skin thickness $a \sim 0.5$ fm in the above for ^{136}Xe on ^{208}Pb is appropriate. Using this choice with Eq. (5) in our folding model leads to partial cross sections that are as much as ~2% larger (depending on the final state) for ^{12}C targets, and less than ~0.2% larger for ^{208}Pb targets, as compared to those obtained using the framework described in Ref. [13]. Along with the geometry of the colliding nuclei, the impact-parameter dependence of the excitation probabilities, especially when including in an approximate way the nuclear form factor as described above, leads to suppression of the target charge dependence of the excitation probabilities, and hence the cross-section ratios, from the pure Z_T^{2n} scaling expected from the Weizsäcker-Williams number spectra.

The numerical integration was carried out from the particle (neutron) threshold to 75 MeV, so that all of the decay strength of ^{136}Xe into the $4n$ channel was included. Considerable strength into the $^{136}\text{Xe} \rightarrow 5n + {}^{131}\text{Xe}$ channel exists near and above 75 MeV. The calculations were not carried out far enough to cover the $5n$ channel in part in the interest of limiting the necessary computing time, but also because the presence of multiple excitations is clearly reflected in the $3n$ and $4n$ channels, as described below.

The standard statistical model, in the form of the computer code CASCADE [37], is used to predict the probabilities for the variety of fragmentation channels that follow the (multiple) excitation. A version of this code that includes proper treatment of the isospin and parity involved in the nuclear decay has been developed [38], but was not used here to allow comparison with the calculations performed [13] for ^{28}Si at AGS energies. We note, however, that the treatment of isospin and parity may have a significant effect on calculation of the strengths for specific final states following EM excitations of the (single) GDR—especially for $1p$, $1n$, and 1α decays from the GDR in ^{28}Si.

The use of CASCADE assumes complete mixing of the produced states into the compound nucleus. The validity of the application of the statistical model in this context can be investigated by comparison to available experimental data. We stress, however, that the specific modelling of the decay step of the reaction does not affect the strategy, described below and mentioned in Ref. [13], that can be used to make inferences about the (multiple) excitation step in the reaction. The decay probabilities leading to exclusive final states following single and multiple excitations do not influence the ratios of cross sections.

IV. RESULTS

In this section, the results of the calculations of the (multiple) $E1$ excitation of ^{136}Xe at a laboratory kinetic energy of 0.65 GeV/nucleon are presented and compared to results for lighter projectiles at higher beam energies. All input parameters not specifically described in Sec. III are taken from Ref. [13].

The differential cross sections $d\sigma^{(n)}/dE$ for the electromagnetic excitation of ^{136}Xe by natural C, Al, Cu, Sn, Pb, and U targets are shown in Fig. 6. The nth-order cross sections are peaked at excitation energies given by nE_{GDR}, similar to the results described in Ref. [13], with overall shapes that reflect the relative smoothness of the

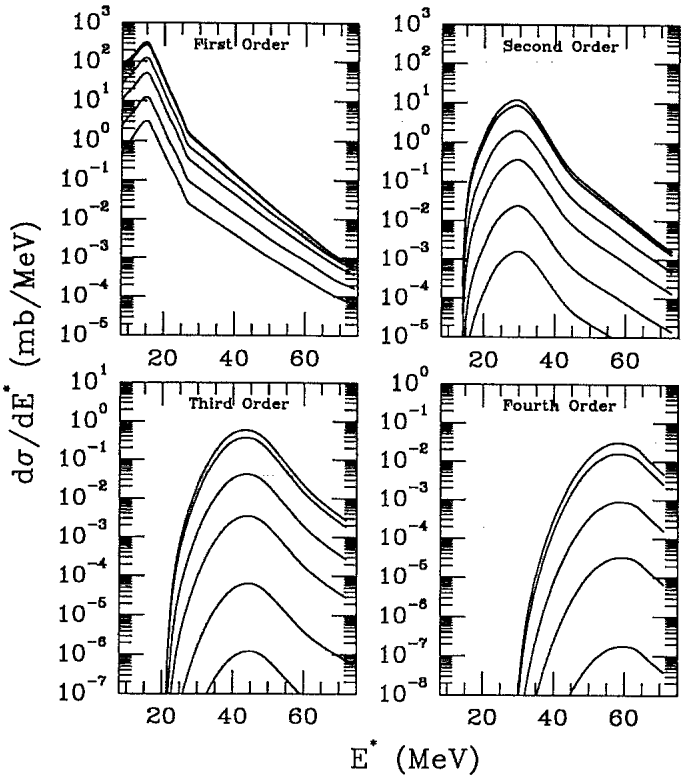

FIG. 6. The calculated differential cross sections for first-, second-, third-, and fourth-order $E1$ excitations of ^{136}Xe at a laboratory kinetic energy of 0.65 GeV/nucleon by C, Al, Cu, Sn, Pb, and U targets. The fourth-order differential excitation cross section by C targets is not shown for clarity.

experimental photoabsorption cross section as compared to those measured for light nuclei.

The cross sections computed using the statistical model approach for the fragmentation of ^{136}Xe into exclusive final states following nth-order $E1$ excitations are presented in Table I. The dominant channels are those involving the evaporation of several neutrons, the population of charged final states occurring with cross sections that are less than a few microbarns. The sum of these—the total cross sections into exclusive final states including up to fourth order, purely $E1$, excitations—are given in Table II. The partial cross sections for absorptions into isoscalar and isovector GQR's obtained using the parametrizations for the GQR photoabsorption cross sections based on the systematics of the available experimental data are included with the $E1$ excitation cross sections in Table III. The absorption of (equivalent) photons into GQR's is thus an important source of fragmentation strength, most importantly for the $1n$, $2n$, and $3n$ decay channels from ^{136}Xe. The absorption of $E2$ photons is of lesser importance for the $^{136}\text{Xe}^* \rightarrow {}^{132}\text{Xe} + 4n$ decay channel, which is also visible in Figs. 3 and 4.

The ratios of the differential nth-order cross sections for the Coulomb fragmentation of ^{136}Xe predicted by our calculations are shown in Fig. 7. The ratios of cross sections into identified final states, the $^{136}\text{Xe} \rightarrow 1n$, $2n$, $3n$, and $4n + {}^{X}\text{Xe}$ decay channels, labeled by the calculated threshold Q values for each, are shown in Fig. 8. The channels in Fig. 8 are labeled by their threshold Q value for comparison with experimental data for which the excitation energy E^* is not measured.

The ratios obtained by dividing the calculated cross sections from a ^{208}Pb target by those from a ^{12}C target when we include the higher-order excitations show an enhancement *of approximately a factor of 10* over that expected from purely first-order excitations. This enhancement decreases to about a factor of 2 when the Pb target cross sections are divided by those for heavier targets. This should be compared with results obtained for the AGS and the SPS [13], where the enhancement in the Pb/C cross-section ratios is only slightly larger than 10% at AGS energies, and less than 5% at the SPS.

V. SUMMARY AND CONCLUSIONS

In this paper we have expanded on the results of previous investigations into the multiple electromagnetic exci-

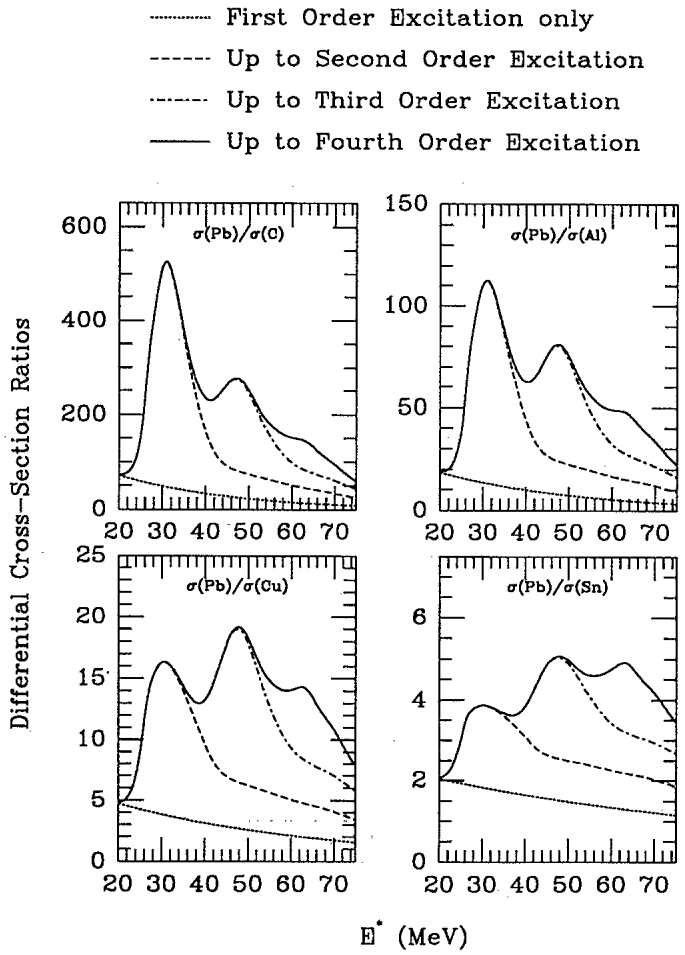

FIG. 7. The ratios of differential total cross sections for the excitation of ^{136}Xe at a laboratory kinetic energy of 0.65 GeV/nucleon obtained from the calculation for Pb targets divided by C, Al, Cu, and Sn targets for each order of excitation up to fourth order.

TABLE I. The cross sections predicted by the folding model of Ref. [13] for purely first-, second-, third-, and fourth-order $E1$ excitation and subsequent statistical decay of ^{136}Xe at a laboratory kinetic energy of 0.65 GeV/nucleon.

Final state	$-Q$ (MeV)	σ(C) (mb)	σ(Al) (mb)	σ(Cu) (mb)	σ(Sn) (mb)	σ(Pb) (mb)	σ(U) (mb)
			First order				
^{135}Xe+1n	8.0	13.7	56.4	234.2	582.0	1279.5	1520.9
^{134}Xe+2n	14.4	6.6	26.1	103.4	245.5	513.2	601.4
^{133}Xe+3n	23.0	0.15	0.54	1.9	3.9	7.3	8.2
^{132}Xe+4n	29.4	0.04	0.13	0.40	0.76	1.3	1.4
			Second order				
Final state	$-Q$ (MeV)	σ(C) (μb)	σ(Al) (μb)	σ(Cu) (mb)	σ(Sn) (mb)	σ(Pb) (mb)	σ(U) (mb)
^{135}Xe+1n	8.0	0.03	0.5	0.008	0.048	0.24	0.33
^{134}Xe+2n	14.4	4.7	72.2	1.1	6.4	29.1	40.6
^{133}Xe+3n	23.0	11.2	164.1	2.4	13.0	56.0	76.8
^{132}Xe+4n	29.4	1.7	24.1	0.33	1.6	6.6	8.8
			Third order				
Final state	$-Q$ (MeV)	σ(C) (nb)	σ(Al) (nb)	σ(Cu) (μb)	σ(Sn) (μb)	σ(Pb) (mb)	σ(U) (mb)
^{135}Xe+1n	8.0	0.0	0.0	0.0	0.0	0.0	0.0
^{134}Xe+2n	14.4	0.019	1.1	0.06	0.88	0.009	0.014
^{133}Xe+3n	23.0	1.6	91.9	5.2	67.6	0.63	1.0
^{132}Xe+4n	29.4	9.9	528.8	28.4	347.3	3.1	4.9
			Fourth order				
Final state	$-Q$ (MeV)	σ(C) (nb)	σ(Al) (nb)	σ(Cu) (nb)	σ(Sn) (nb)	σ(Pb) (μb)	σ(U) (μb)
^{135}Xe+1n	8.0	0.0	0.0	0.0	0.0	0.0	0.0
^{134}Xe+2n	14.4	0.0	0.0	0.0	0.02	0.0	0.0
^{133}Xe+3n	23.0	0.0	0.0	0.48	14.6	0.30	0.57
^{132}Xe+4n	29.4	0.0	0.18	36.5	1055.9	20.3	38.8

TABLE II. The total cross sections predicted by the folding model of Ref. [13] for up to fourth-order $E1$ excitation and subsequent statistical decay of ^{136}Xe at a laboratory kinetic energy of 0.65 GeV/nucleon.

Final state	$-Q$ (MeV)	σ(C) (mb)	σ(Al) (mb)	σ(Cu) (mb)	σ(Sn) (mb)	σ(Pb) (mb)	σ(U) (mb)
^{135}Xe+1n	8.0	13.7	56.4	234.2	582.0	1279.7	1521.2
^{134}Xe+2n	14.4	6.6	26.2	107.6	251.9	542.4	642.1
^{133}Xe+3n	23.0	0.16	0.70	4.3	17.0	63.9	86.0
^{132}Xe+4n	29.4	0.04	0.15	0.76	2.8	10.9	15.2

TABLE III. The total cross sections predicted by the folding model of Ref. [13] for up to fourth-order $E1$ and first-order $E2$ excitation, which includes excitations of isoscalar and isovector GQR's, and subsequent statistical decay of ^{136}Xe at a laboratory kinetic energy of 0.65 GeV/nucleon.

Final state	$-Q$ (MeV)	σ(C) (mb)	σ(Al) (mb)	σ(Cu) (mb)	σ(Sn) (mb)	σ(Pb) (mb)	σ(U) (mb)
^{135}Xe+1n	8.0	17.8	72.0	294.7	726.7	1597.2	1900.3
^{134}Xe+2n	14.4	8.0	31.2	123.1	293.8	629.1	743.8
^{133}Xe+3n	23.0	0.43	1.7	7.6	24.1	77.6	101.9
^{132}Xe+4n	29.4	0.06	0.22	0.97	3.2	11.7	16.0

tation of GDR states in relativistic nuclei. Three physical processes also contribute to the cross sections—first-order $E1$, GQR, and nuclear excitations—imposing a strong "background" atop the predicted multistep GDR excitation strengths.

The strength of first-order $E1$ excitations leading to excitation energies $E^* \sim 2E_{\mathrm{GDR}}$, where double-GDR excitations are predicted to occur, is suppressed by the use of beam energies on the order of ~1 GeV/nucleon. However, two other processes become increasingly important at low beam energies, from the Bevalac or SIS accelerators, for example, as compared to higher beam energies available from the AGS or SPS.

The excitation and decay of giant quadrupole resonances, in particular the isovector GQR, contributes fragmentation strength in the same region of excitation energy covered by multiple $E1$ excitations. These GQR absorptions provide non-negligible decay strength into exclusive final-state channels, so great care is required if the search for multiple excitations is to occur by the inspection of experimentally measured dissociation cross sections alone.

In addition, excitations resulting from peripheral nuclear interactions are most important relative to electromagnetic excitations of any order at low beam energies. The quality of the separation of the electromagnetic and nuclear components, a matter demanding consideration both during the on-line data collection and in the final analysis, is of *crucial* importance for the isolation of multiple electromagnetic excitations.

Considerable insight into the character of measured experimental data is obtained by the formation of the ratios of either exclusive partial cross sections or differential cross sections measured for projectile excitations by two different target species. These ratios of cross sections measured using targets of very different charges are sensitive indicators of the presence of multiple excitations whether they involve purely $E1$ photons, purely $E2$ photons, or some combination of $E1$ and $E2$ photons, but are suppressed by fragmentation strength resulting from nuclear interactions. Thus, while our estimates indicate that the integrated strength of isoscalar and isovector GQR excitations exceeds that expected for double-GDR excitations, such strength does not interfere with any experimental assessment of the presence of multiple GDR excitations involving cross-section ratios.

At low projectile energies, the overall electromagnetic excitation cross sections are small, especially with respect to the essentially beam-energy-independent strength of peripheral nuclear interactions. The nuclear component may well dominate the event sample at low beam energies to such an extent that no firm statement concerning the presence of multiple electromagnetic excitations will be possible. The number spectra of $E2$ (equivalent) photons exceeds that for $E1$ photons at low beam energies, so GQR excitations provide sizable absorption strength in this case. Higher beam energies have the advantage of larger overall electromagnetic excitation strengths, especially relative to nuclear excitations, as well as weaker spectra of $E2$ photons relative to $E1$ photons and the advantages in event characterization provided by stronger kinematic focusing, but suffer from relatively smaller enhancements in cross-section ratios.

For a given beam energy, the excitation of heavy projectiles like ^{136}Xe leads to larger overall cross sections as compared to those for light ones like ^{28}Si, due to the lower mean position of the GDR in heavy nuclei coupled with the $1/E_\gamma$ dependence of the various spectra of (equivalent) photons. For this reason, the total higher-order excitation cross sections are also larger than those for light nuclei. However, the possibility of the measurement of very large amplitude collective final states that may result from the absorption of several photons in the GDR is more promising in light nuclei [19].

Experimental verification of the occurrence of multistep electromagnetic excitations in relativistic nucleus-nucleus collisions would allow exciting new investigations into the character of atomic nuclei following the measurement of their response to the extreme conditions imposed by multiple excitations. In addition, if the existence of multiple GDR states can be experimentally ver-

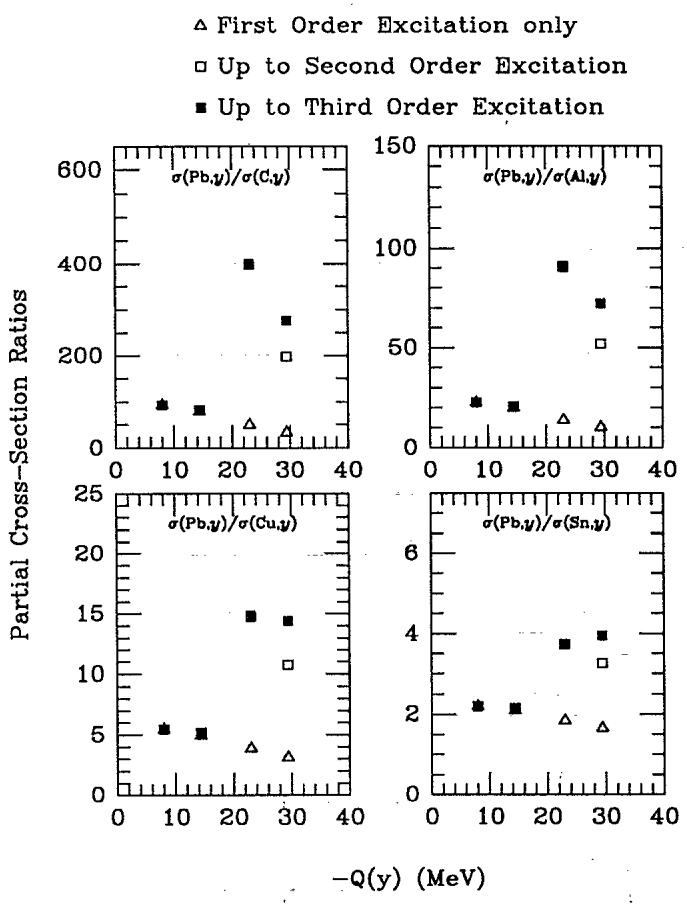

FIG. 8. The ratios of partial cross sections into the $1n$, $2n$, $3n$, and $4n$ decay channels of ^{136}Xe projectiles at laboratory kinetic energies of 0.65 GeV/nucleon. Here, the partial cross sections, obtained by the calculation, for Pb targets are divided by C, Al, Cu, and Sn targets for each order of excitation up to fourth order.

ified, they might provide an efficient mechanism for the production of final states of many neutrons with little relative temperature—opening the door for renewed investigations [13, 24] into possibly bound or metastable multineutron [39] systems.

One of the authors (W.J.L.) would like to thank Dr. H. Emling for interest in this work, and Dr. H. Takai, Dr. J.W. Norbury, and Dr. M.N. Harakeh for helpful discussions. This work was supported in part by the National Science Foundation.

[1] J. Barrette *et al.*, Phys. Rev. C **41**, 1512 (1990).
[2] X. Artru and G.B. Yodh, Phys. Lett. **40B**, 43 (1972).
[3] H.H. Heckman and P.J. Lindstrom, Phys. Rev. Lett. **37**, 56 (1976); G.D. Westfall, L.W. Wilson, P.J. Lindstrom, H.J. Crawford, D.E. Greiner, and H.H. Heckman, Phys. Rev. C **19**, 1309 (1979); D.L. Olsen, B.L. Berman, D.E. Greiner, H.H. Heckman, P.J. Lindstrom, G.D. Westfall, and H.J. Crawford, *ibid.* **24**, 1529 (1981); D.L. Olsen, B.L. Berman, D.E. Greiner, H.H. Heckman, P.J. Lindstrom, and H.J. Crawford, *ibid.* **28**, 1602 (1983); D.L. Olsen, M. Baumgartner, D.E. Greiner, P.J. Lindstrom, T.J.M. Symons, R. Wada, M.L. Webb, B.L. Berman, H.J. Crawford, and J.M. Engelage, *ibid.* **44**, 1862 (1991).
[4] M.T. Mercier, J.C. Hill, F.K. Wohn, and A.R. Smith, Phys. Rev. Lett. **52**, 898 (1984); M.T. Mercier, J.C. Hill, F.K. Wohn, C.M. McCollough, M.E. Nieland, J.A. Winger, C.B. Howard, S. Renwick, D.K. Matheis, and A.R. Smith, Phys. Rev. C **33**, 1655 (1986); J.C. Hill, F.K. Wohn, J.A. Winger, and A.R. Smith, Phys. Rev. Lett. **60**, 999 (1988); J.C. Hill, F.K. Wohn, J.A. Winger, M. Khayat, K. Leininger, and A.R. Smith, Phys. Rev. C **38**, 1722 (1988); A.R. Smith, J.C. Hill, J.A. Winger, and P.J. Karol, *ibid.* **38**, 210 (1988); J.C. Hill, F.K. Wohn, J.A. Winger, M. Khayat, M.T. Mercier, and A.R. Smith, *ibid.* **39**, 524 (1989).
[5] C. Brechtmann and W. Heinrich, Z. Phys. A **330**, 407 (1988); C. Brechtmann and W. Heinrich, *ibid.* **331**, 463 (1988); C. Brechtmann, W. Heinrich, and E.V. Benton, Phys. Rev. C **39**, 2222 (1989).
[6] I. Tanihata, Nucl. Phys. **A488**, 113 (1988).
[7] Y.D. He, P.B. Price, and W.T. Williams, Phys. Lett. **252B**, 331 (1990).
[8] N. Ardito *et al.*, Europhys. Lett. **6**, 131 (1988); L. Ramello, Z. Phys. C **38**, 73 (1988); P.B. Price, Ren Guoxiao, and W.T. Williams, Phys. Rev. Lett. **61**, 2193 (1988); G. Singh, K. Sengupta, and P.L. Jain, Phys. Rev. C **41**, 999 (1990).
[9] G. Baroni *et al.*, Nucl. Phys. **A516**, 673 (1990).
[10] S. Mordechai *et al.*, Phys. Rev. Lett. **61**, 531 (1988); S. Mordechai *et al.*, Phys. Rev. C **41**, 202 (1990); S. Mordechai *et al.*, *ibid.* **43**, 1509 (1991).
[11] Ph. Chomaz *et al.*, Z. Phys. A **318**, 41 (1984); Ph. Chomaz *et al.*, *ibid.* **319**, 167 (1984); Ph. Chomaz and D. Vautherin, Phys. Lett. **139B**, 244 (1984).
[12] F.E. Bertrand *et al.*, Phys. Rev. C **35**, 111 (1987), and references therein.
[13] W.J. Llope and P. Braun-Munzinger, Phys. Rev. C **41**, 2644 (1990).
[14] E. Fermi, Z. Phys. **29**, 315 (1924); C.F. Weizsäcker, *ibid.* **88**, 612 (1934); E.J. Williams, Phys. Rev. **45**, 729 (1934); V.M. Budnev, I.F. Ginzburg, G.V. Meledin, and V.G. Serbo, Phys. Rep. C **15**, 183 (1975).
[15] J.D. Jackson, *Classical Electrodynamics*, 2nd Ed. (Wiley, New York, 1975), Chap. 15.
[16] B. Hoffman and G. Baur, Phys. Rev. C **30**, 247 (1984).
[17] J. Ahrens *et al.*, Nucl. Phys. **A251**, 479 (1975); J. Ahrens, *ibid.* **A446**, 229 (1985); J. Ahrens, J. Eyink, A. Hegerath, K.G. Hilger, B. Mecking, G. Nöldeke, and H. Rost, Phys. Lett. **98B**, 423 (1981).
[18] B.L. Berman, Lawrence Livermore Laboratory Report No. UCRL-75694 (1974).
[19] G. Baur and C.A. Bertulani, Phys. Rep. **163**, 299 (1988).
[20] J.S. Levinger, Phys. Rev. **84**, 43 (1951).
[21] J.W. Norbury, Phys. Rev. C **40**, 2621 (1989); **41**, 372 (1990); **42**, 711 (1990); **42**, 2259 (1990).
[22] R. Fleischhauer and W. Scheid, Nucl. Phys. **A493**, 583 (1989); R. Fleischhauer and W. Scheid, *ibid.* **A510**, 817 (1990).
[23] C. Pruneau and H. Takai (unpublished).
[24] P. Braun-Munzinger *et al.*, proposal for the BNL-AGS, Brookhaven National Laboratory Report, 1985 (E814 Collaboration).
[25] H. Emling *et al.*, proposal for the GSI-SIS (unpublished).
[26] W.D. Myers, W.J. Swiatecki, T. Kodama, L.J. El-Jaick, and E.R. Hilf, Phys. Rev. C **15**, 2032 (1977).
[27] F.E. Bertrand and J.R. Beene, *Proceedings of the 1989 International Nuclear Physics Conference* (World Scientific, Singapore, 1990), p. 397.
[28] A. Bohr and B. Mottleson, *Nuclear Structure* (Benjamin, Reading, 1975), Vol. II, Ch. 6.
[29] F.E. Bertrand, Annu. Rev. Nucl. Sci. **26**, 457 (1976), and references therein; A. Van der Woude, in *Giant Resonances*, edited by J. Speth (World Scientific, Singapore, 1990), Ch. 2, and references therein.
[30] P. Paul, MPI-Heidelberg Report No. MPI H-1975-V22.
[31] C.J. Benesh, B.C. Cook, and J.P. Vary, Phys. Rev. C **40**, 1198 (1989).
[32] P.J. Karol, Phys. Rev. C **11**, 1203 (1975).
[33] A.J. Cole, Z. Phys. A **322**, 315 (1985); Phys. Rev. C **35**, 117 (1987); A.J. Cole, R. Cherkaoui, and J. Alarja, *ibid.* **40**, 1265 (1989).
[34] H. Überall, *Electron Scattering from Complex Nuclei* (Academic, New York, 1971), Vols. A and B.
[35] D.V. Bugg, D.C. Salter, G.H. Stafford, R.F. George, K.F. Riley, and R.J. Tapper, Phys. Rev. **146**, 980 (1966); Particle Data Group, Phys. Lett. B **239**, 1 (1990).
[36] J.W. Norbury and L.W. Townsend, Phys. Rev. C **42**, 1775 (1990).
[37] F. Pühlhofer, Nucl. Phys. **A280**, 267 (1977).
[38] CASCIP—an extended version of the code CASCADE—M.N. Harakeh, private communication.
[39] J. Cerny, R.B. Weisenmiller, N.A. Jelley, K.H. Wilcox, and G.J. Wozniak, Phys. Lett. **53B**, 247 (1974); L.M. Delves and A.C. Phillips, Rev. Mod. Phys. **41**, 497 (1969) and references therein; S. Fiarman and W.E. Meyerhof, Nucl. Phys. **A206**, 1 (1973) and references therein.